Modulating Inflammation in Monocytes Using Capillary Fiber Organic Electronic Ion Pumps

Maria S Seitanidou, Robert Blomgran, Giggil Pushpamithran, Magnus Berggren and Daniel Simon

Seitanidou, M. S, Blomgran, R., Pushpamithran, G., Berggren, M., Simon, D., (2019), Modulating Inflammation in Monocytes Using Capillary Fiber Organic Electronic Ion Pumps, *Advanced Healthcare Materials*, 8(19), 1900813. https://doi.org/10.1002/adhm.201900813

Original publication available at:
https://doi.org/10.1002/adhm.201900813

Modulating inflammation in monocytes using capillary fiber organic electronic ion pumps

Maria Seitanidou[1], Robert Blomgran[2], Giggil Pushpamithran[2], Magnus Berggren[1], Daniel T. Simon[1]
1. Laboratory of Organic Electronics, Department of Science and Technology, Linköping University, 60174 Norrköping, Sweden
2. Division of Medical Microbiology, Department of Clinical and Experimental Medicine, Linköping University, 581 85 Linköping, Sweden

Abstract

Organic electronic ion pump (OEIP) delivers ions and drugs from a source, through a charge selective membrane, to a target upon an electric bias. Miniaturization of this technology is crucial and will provide several advantages, ranging from better spatiotemporal control of delivery to reduced invasiveness for implanted OEIPs. To miniaturize OEIPs, we have developed new configurations based on glass capillary fibers that are filled with an anion exchange membrane (AEM). Fiber capillary OEIPs can be easily implanted in proximity to targeted cells and tissues. Here, we demonstrate the efficacy of such a fiber capillary OEIP for modulation of inflammation in human monocytes. The devices were located on inflammatory monocytes and local delivery of salicylic acid (SA) was initiated. Highly localized SA delivery results in a significant decrease in cytokine (TNFα and IL-6) levels after lipopolysaccharide (LPS) stimulation. Our findings – the first use of such capillary OEIPs in mammalian cells or systems – demonstrate the utility of the technology for optimizing transport and delivery of different therapeutic substances at low concentrations, with the benefit of local and controlled administration that limits the adverse effect of oral/systemic drug delivery.

Keywords

Organic electronics, drug delivery, electrophoresis, iontronics, ion exchange membrane, bioelectronics, inflammation, cytokines, capillary fiber.

Introduction

Organic bioelectronics can be considered as a technological solution to a variety of diagnostic and therapeutic purposes due to its unique ability to translate signals between biology and technology.[1–4]

During the past 10 years organic bioelectronic systems capable of recording and regulating biological functions have been demonstrated to overcome many of the limitations of pharmaceutical or traditional bioelectronic techniques.[5,6] This technology can serve as an efficient tool for an application such as biosensing[7–9], electrophysiological recording[10], and drug delivery[11–13]. Organic electronic ion pumps (OEIPs) are a primary example of organic bioelectronics combining electronic and ionic properties of organic electronics materials[14–16] to enable release, via electronic addressing, of ionic-biochemical signals for biological applications. OEIPs operate as an "iontronic" resistors[17–19] and can be used to electrophoretically deliver charged species through a cation- or anion-exchange membrane (CEM or AEM), resulting in high spatiotemporal delivery resolution and high dosage precision (one electron per delivered monovalent ion).[14] In recent years, these electrophoretic delivery devices have been used to trigger cell signaling *in vitro*[1,20], to control epileptiform activity in brain slice models[21–23], to effect sensory function *in vivo*[19], to suppress pain sensation in awake animals[17], and to modulate plant physiology[24,25]. OEIP devices based on glass capillary fibers offer several design advantages for use in freestanding or implantable geometries. OEIPs fiber capillaries, in contrast to planar OEIPs devices, provide less water uptake inside the channel providing a large ion-transport cross-section with high ionic conductivity, which allow transport of relatively large ions such as drugs and neurotransmitters.[26,27] These devices can furthermore be more easily implanted or located in proximity to targeted cells, tissues, or organs.

In the present work, we demonstrate OEIPs based on glass capillary fibers that are filled with a polyelectrolyte (polycationic AEM). The AEM is characterized by a high concentration of fixed positive charges that allows for the selective transport of negative ions while blocking coions from drifting in the opposite direction. Non-fixed mobile ions with the same charge with the fixed charges of ion exchange membrane (IEM) are referred to as coions while ions with opposite charge are referred to as counterions. The permselectivity, according to Donnan exclusion, holds if the ionic concentrations in the adjacent electrolytes are considerably lower than the fixed charge concentration of the AEM.[28] The potential gradient, and associated current through the OEIPs fiber capillaries, is established by applying

a potential difference between electrodes (Ag/AgCl) applied in the source and target solutions.[27] The polarizable electrodes in this study comprise a thin film of the conducting polymer blend poly(3,4-ethylenedioxythiophene) polystyrene sulfonate (PEDOT:PSS) on a polyethylene terephthalate (PET) substrate with additional Ag/AgCl to promote good contact. The capillary "ion channel" of the OEIP was filled with the polycation poly[2-(acryloyloxy) ethyl]trimethylammonium chloride (AETMAC), cross-linked with polyalcohol polyethylene glycol (PEG) (Figure 1).

We used acetylsalicylic acid (ASA) and salicylic acid (SA) drugs as the model delivery substances since ASA and its active component (SA) are arguably one of the world's oldest and best-known pharmaceutical drugs. ASA is often used to treat pain, fever, or inflammatory diseases and is classified as a nonsteroidal anti-inflammatory drug (NSAID).[29] Inflammation is a major risk factor for many diseases.[30] It is a complex physiological defense mechanism in the body caused by several physical reactions that are triggered by the immune system in response to a physical injury or infection.[31] Further, long-term use of ASA at low doses is known to prevent heart attack[32,33] , stroke[34], and blood clot formation[35] in high-risk patients. ASA is a prodrug and is rapidly hydrolyzed in the body to form SA, which is the compound that is primarily responsible for the pharmacological activity of the drug. In this study, we investigated the effects of well-defined and targeted doses of ASA and SA delivered locally to monocytes. Lipopolysaccharide (LPS) was used to model inflammation as it stimulates inflammatory cells of the immune system.[36–38] LPS is a pathogenic endotoxic component in the outer membrane of gram-negative bacteria and can disturb the balance between immunity and inflammatory response.[39] LPS stimulation triggers production of pro-inflammatory cytokines such as tumor necrosis factor alpha (TNFα) and interleukin 6 (IL-6), which mediate septic shock and acute lung inflammation.[40,41] Monocytes from healthy blood donors were used to investigate inflammatory responses triggered by LPS and the anti-inflammatory effects of SA, as modulated by a controlled delivery using capillary OEIPs.

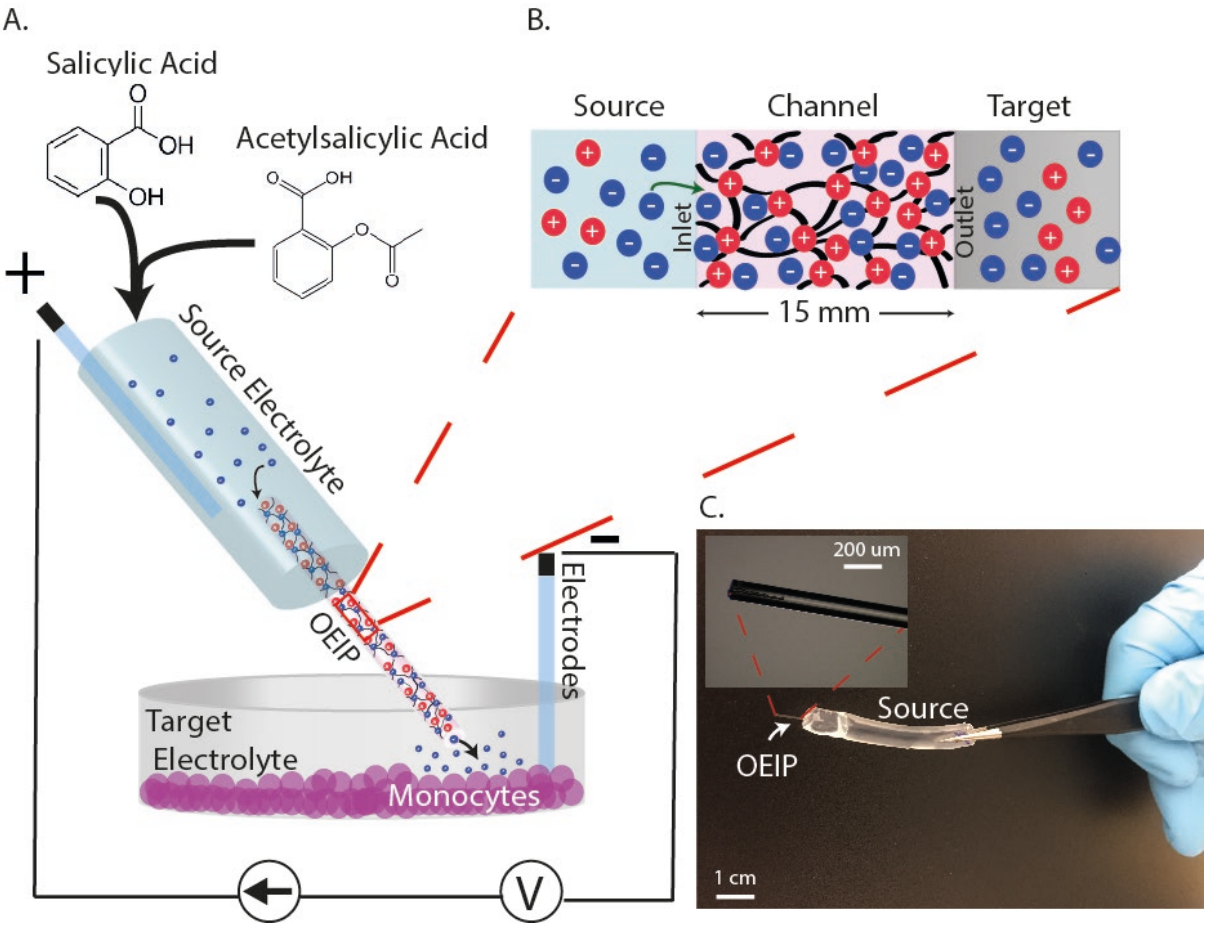

Figure 1: ***(A)*** *Experimental setup.* ***(B)*** *Schematic illustration of AEM.* ***(C)*** *Photograph of OEIP fiber capillary device.*

Results and Discussion

Capillary OEIPs were characterized by loading the channel with aqueous electrolyte containing the drug (10 mM SA (aq) or 10 mM ASA (aq)) and were then pH-adjusted by the addition of KOH to pH 7 (Supplementary Figure S1). A constant 1 V potential was then applied to the source electrode for 17 hours, with the target electrode grounded, and the resulting current was recorded. The steady-state current (10000 sec) for SA delivery was slightly higher than for ASA (Figure 2A). The ionic conductivity depends on the mobility characteristics of the molecules.[42] However, the size and the diffusion coefficient had similar values for ASA and SA (diffusion coefficient = 10^{-6} cm^2s^{-1}).[43,44] To investigate the effect of SA and ASA delivery on the target electrolyte, the resulting target electrolytes were collected, and a quantitative determination of concentrations was performed using UV-Vis spectrometry. According to the UV analysis, the absorption peak of ASA was shifted to lower wavelength and was

observed at 290 nm, identical to the absorption point of SA (Figure 2B).[45] The target electrolytes were quantified using a salicylate enzyme-linked immunosorbent assay (ELISA) kit. Although the source electrolyte was loaded with ASA, the ELISA quantification indicated that the delivered molecule was SA (Figure 2C). With capillary OEIPs, irregularities in substance delivery have been observed due to concentration polarization which in turn causes electric field enhanced water dissociation at the ion channel inlet (in the source electrolyte).[27] This phenomenon is particularly intense at low concentrations of drugs and for relatively larger (low diffusion constant) molecules. To investigate this phenomenon a voltage was sourced within the range of 0-1 V and the currents were recorded at a scan rate of 5 mVs^{-1} for different ASA concentrations (100 mM and 10 mM). The I-V curves show three characteristic regions which are most pronounced for the relatively lower electrolyte concentration (10 mM). From the results given in Figure 2D, the limiting current depends on the ASA concentration and is reached at 0.3 V at the lower concentration, characterized by a plateau. Above the limiting current plateau, the linear region increases in the I-V characteristics and is referred to as the over-limiting current region. From a device perspective, it is important to understand the nature of the over-limiting current. Water dissociation occurs above 0.8 V (linear region) and generates protons at the capillary inlet, leading to protonation of ASA. According to this reaction, ASA is hydrolyzed to SA at the inlet, and SA is more quickly transported through the ion channel (AEM) in comparison to ASA. Another process that promotes ASA hydrolysis is the pH decrease in the source electrolyte due to the active delivery of ASA anions into the target electrolyte as the potential is applied. Taken together, these factors indicate indicate that the steady current decrease for ASA (30 nA) in Figure 2A is related to the limiting current level in Figure 2D. Above this level, water dissociation occurs, protonating the ASA. These characteristics drove us to choose SA as the drug for delivery, avoiding the ASA delivery limitations.

The ion transport and the permselectivity (selectivity toward transport of cations or anions) is strongly dependent on the concertation of fixed charge concentration of the channel. To achieve the most efficient ion transport, the fixed charge concentration of the channel should be significantly higher than that of the surrounding electrolyte concentrations. Additionally, it is important to determine the fixed

charge concentration of the channel to approximate and specify the operating point at which SA delivery occurs. To this end, we estimated the fixed charge concentration by applying 1.7 μA (0.5 mC) every 5 min over the course of 30 min for 10 mM SA (aq) source electrolyte. Figure 2E shows the amount of SA delivered to the target over the course of these 0.5 mC pulses. The first two data points correspond to electrophoretically driven ion exchange, where each fixed charge group in the channel is compensated by a SA anion. When all the fixed charge sites in the channel are compensated by SA, the resistance of the channel reaches a steady-state value. In this case, the steady-state value corresponds to 1 mC of fixed charge. Using the channel geometry (25 μm diameter, 15 mm length), the equation $C = Q/(F \times V)$ gives 1.4 M of fixed charge, where Q is the total charge (1 mC), F is Faraday's constant, and V is the volume of the channel. These measurements indicate the delivery time to fill in the channel before SA delivery, and led us to apply 100 nA of constant current for 2.5 hours (*i.e.*, 1 mC) to fill the channel before each characterization step.

As a final electrical characterization step, we aimed at identifying the optimum current range for which the highest SA delivery efficiency is reached. The system was operated by applying different currents (10 nA, 50 nA, 100 nA, and 200 nA) between the source and target electrodes for 1.5, 3, 6, and 20 hours using a 10 mM SA (aq) source electrolyte while recording the voltage. The devices were operated in a target solution of 10 mM KCl(aq). To determine the efficiency of the devices, chemical quantification was performed. The efficiency of capillary OEIP transport was defined as the ratio between the number of intended SA molecules transported into the target reservoir (according to chemical quantification by sampling the target electrolyte after delivery) to the number of electrons recorded in the driving circuit (integrated current). Typically, relatively lower current resulted in higher SA delivery efficiency (Figure 2F). The efficiency was 85% when applying 10 nA for 20 hours and when applying 50 nA for 6 hours. Figure 2F shows that for short delivery time (1.5 hours) the efficiency was consistently lower, likely due to the anion transport being dominated by OH^-. Applying higher current (100 nA and 200 nA), the efficiency again was consistently lower, due to the breakdown of the membrane's charge selectivity (Figure 2F). This phenomenon was observed due to the high ionic concentrations resulting from

concentration polarization in the channel void. From the fabrication step, the channel material (AETMAC) doesn't extend all the way to the end of capillary outlet, creating a "void" at the end of the channel with the target electrolyte filling this void. A local ionic concentration at the channel-electrolyte interface increases as SA reaches the outlet, decreasing the membrane selectivity.[26] High operational currents exacerbate this effect and lead to more observable breakdown of the membrane's selectivity. This breakdown leads to backflow of anions from target electrolyte towards the source electrolyte, further decreasing the delivery efficiency. The concentration polarization effect can be prevented by applying lower currents, resulting in an improved pumping efficiency. These lower currents still result in biologically relevant concentrations of delivered drugs (as shown below).

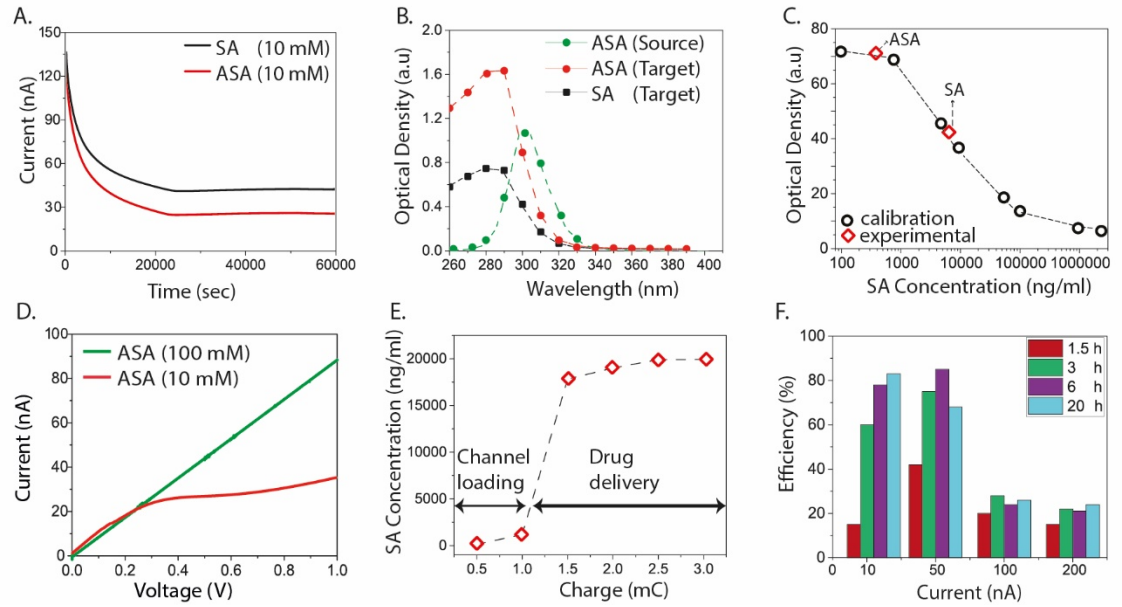

Figure 2: Electrical characterization of fiber capillaries. ***(A)*** *Current vs time for delivery from 10 mM ASA (aq) and 10 mM SA (aq) source electrolytes at 1 V bias.* ***(B)*** *Absorbance spectra of target electrolyte before and after ASA and SA delivery.* ***(C)*** *Quantification of SA and ASA delivery according to SA standard curve.* ***(D)*** *Experimental I-V curves with the three characteristic regions of ASA delivery at different concentrations (100 mM, 10 mM) in the range 0-5 V scanned at a rate of 5 mVs^{-1}.* ***(E)*** *Amount of SA delivered to the target as a function of sequential 1.7 µA pulses, measured every 5 min.* ***(F)*** *Dependence of SA delivery efficiency on the applied current and delivery duration.*

In order to demonstrate the ability of the capillary OEIPs to deliver SA and ascertain anti-inflammatory effect *in vitro*, SA was first manually added by pipette at different concentrations (1, 10, 100, 300 µM)

to human primary monocytes with simultaneous 0.1 ng/ml LPS stimulation. LPS triggers a strong pro-inflammatory response in human monocytes. The anti-inflammatory effect of SA at different concentrations was estimated by quantifying the LPS-induced levels of the pro-inflammatory cytokines TNFα and IL-6. Quantification of TNFα and IL-6 levels were determined after 1.5, 3, 6, and 20 hours after LPS stimulation. Figure 3A shows the levels of IL-6 and TNFα after the addition of SA at different concentrations and at different collection times after LPS stimulation. After 6 hours of LPS stimulation the level of IL-6 reached 1 ng/ml and the level of TNFα peaked at 4 ng/ml. The manual addition of SA had a strong impact: 55% reduction of IL-6 and 40% reduction TNFα, depending on the dose of SA. At this 6-hour time point, 10 μM of SA had the most anti-inflammatory effect (in comparison to 1, 100, and 300 μM SA) on both IL-6 and TNFα cytokines. A similar suppressive response by SA was observed after 20 hours of LPS stimulation, resulting in an IL-6 and TNFα reduction of about 40%. For the shorter collection times (1.5 and 3 hours after LPS stimulation), the addition of SA did not present a strong anti-inflammatory effect and the level of IL-6 and TNFα remained constant independent of the SA concentration used.

SA was then electrically delivered via capillary OEIP to the human primary monocytes. We choose to deliver the optimum SA concentration (10 μM) that showed the most inhibitory effect on LPS at 6 and 20 hours (Figure 3A). In order to deliver this amount of SA we applied the corresponding currents of 60 nA for 6 hours (Figure 3B) and 10 nA for 17 hours (Figure 3C). The SA delivery to monocytes was performed in a 37 °C incubator to maintain physiological conditions. After SA delivery the cells were stimulated with 0.1 ng/ml LPS for 6 hours. The sampling of the cell culture medium was performed before and after the 6 h LPS stimulation with and without the SA delivery, and the levels of TNFα and IL-6 were determined.

The results shown in Figure 3B and 3C demonstrate that capillary OEIP delivery of SA prevented LPS-induced inflammation. The LPS-induced IL-6 and TNFα was completely blocked by the 6 h delivery of SA prior to LPS-stimulation (Figure 3B). When comparing the IL-6 and TNFα levels before and after LPS

stimulation without SA delivery, IL-6 reached 2.3±0.24 ng/ml (at least 5.8-fold increase) and TNFα reached 4.7±1.7 ng/ml (at least 20-fold increase), mean±SD of 3 donors. This indicates that LPS triggers a strong pro-inflammatory response in human monocytes, and that the 6 h delivery of SA completely abolished the LPS-induced IL-6 and TNFα response (Figure 3B). Going one step further, we applied a lower current (10 nA) for 17 h to deliver SA to primary monocytes of two individual donors (D1, D2). Again, LPS induced a robust increase in the pro-inflammatory cytokines in the absence of SA delivery, showing an approximate 6-fold increase in both IL-6 and TNFα, with minor difference between the donors. And again, we observed a complete inhibition of IL-6 and TNFα with SA delivery even with this lower current protocol (prolonged SA delivery) (Figure 3C). However, for both donors the prolonged OEIP SA delivery increased the basal levels of IL-6 and TNFα, i.e. before stimulation, but these cytokine levels did not further increase by LPS-stimulation, still indicating the inhibitory capacity of OEIP delivered SA. These results (Figure 3B-C) provide strong evidence that there is a complete inhibition of the LPS-induced response by OEIP delivery of SA, and indicate that even small amounts of delivered SA can significantly affect the cells by blocking the IL-6 and TNFα production and prevent further increase in a scenario of pro-inflammatory cytokine induction. Taken together, these results lead us to conclude that 6 h delivery of SA is enough to prevent pro-inflammatory activation of monocytes, presenting high delivery efficiency (90%), and that prolonged delivery (17 h) have no added benefit.

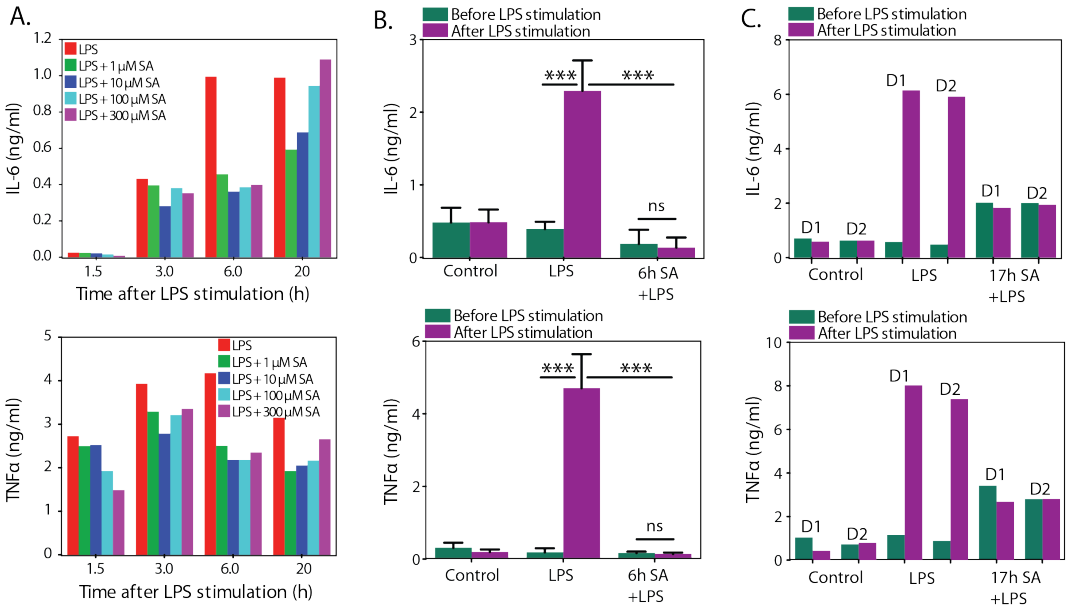

Figure 3: ***(A)*** *IL-6 and TNFα level after LPS stimulation of human monocytes, at different sampling time points and different concentration of SA added together with LPS. IL-6 and TNFα concentration was also measured before and after 6h of LPS stimulation, using the OEIPs to deliver SA (SA delivery) for different periods prior stimulation (B-C).* ***(B)*** *SA (10 mM) was delivered to monocytes for 6 hours and LPS stimulation was performed for 6 hours, and the cytokines measured just before stimulation (as reference) and 6h after stimulation. Showing mean±SD for 3 donors and using repeated measure ANOVA with Tukey post-test for differences between groups; ***, p<0.001; ns, not significant.* ***(C)*** *SA (10 mM) was delivered to monocytes for 17 hours, and the cytokines measured just before stimulation (as reference) and 6h after stimulation. Monocytes in C show the individual results from 2 donors (D1 and D2).*

Methods

OEIP Fiber Capillaries Fabrication

Glass capillary fibers with inner diameter 25 µm and outer diameter 125 µm (Polymicro Technologies, CM Scientific) were cut by hand to a length of 30 cm using a ceramic cleaving stone. The capillaries were provided with a polyimide coating to provide abrasion resistance. The capillaries were soaked in concentrated sulfuric acid to remove the polyimide coating; above 100 °C, the sulfuric acid removes the polyimide under a slow stirring for 20 min. When the polyimide was removed, the glass capillary was rinsed with DI water. A needle adapter was assembled to the capillary using a glue and heat gun and connected vertically, via 5 ml disposable polypropylene syringe, to a nitrogen line fitting for flushing. The syringe reservoir was connected to the nitrogen supply line to give the desired flow rate of the different solvents (1 ml). The first process step was to flush the capillary with nitrogen at 5 bar for 5 min. Then 2 M KOH was flushed through the capillary for 2 hours to allow for etching of the inner surface. This etching step increases the hydrophilicity of the capillary since KOH solution increases the surface silanol concentration: hydroxide ions react with the silanol groups of the silica surface to produce silicate ions.[46] After KOH etching, the capillary was flushed with DI water for 10 min and dried by nitrogen flushing for 5 min. The next process step was silanization. 3-(Trimethoxysilyl)propylmethacrylate (10 wt% in toluene) was flushed for 1 hour followed by drying with nitrogen flushing for 5 min and ethanol flushing for 10 min. Vinylic groups are introduced on the surface of the fused silica capillary and ensure that the polymer is attached covalently to the capillary wall. The silanizing agent reacts with the silanol

group on the glass surface and methacrylic groups are expressed on the surface providing hydrophobic characteristics.[46] The last process step was flushing the acrylate monomer (2-(acryloyloxy)ethyl trimethylammonium chloride (AETMAC), Sigma-Aldrich, M_W 2000, 35 wt %) using a dark syringe tube for 20 min. AETMAC was mixed with polyethylene glycol diacrylate (PEG-DA, M_W 575, 2 wt %) and a photoinitiator (0.5 wt % 2-hydroxy-4'-(2-hydroxyethoxy)-2-methylpropiophenone, Sigma Aldrich) that promotes cross-linking in DI water. Finally, using a UV light (UVS-28 EL Series 8 W, 254 nm) the capillary monomer was polymerized after 10 min. After the polymerization, the capillary was cut into 20 desired device lengths (15 mm) by a fiber cleaver, and these were assembled directly onto heat shrink tubes/reservoirs. The capillary OEIP devices were immersed and stored in 1 mM KCl(aq) electrolyte before use to hydrate the polycatanion membrane.[27]

Electrical Characterization

Ion transport was evaluated via electrical measurements. OEIPs fiber capillaries were characterized by loading the channel with aqueous electrolyte containing the drug of interest (10 mM SA (aq) and 10 mM ASA(aq)). Electrical characterization was performed using a Keithley 2602 SourceMeter (Keithley Instruments Inc.) with custom designed LabVIEW software. The polycation membrane was filled with an ASA or SA source electrolytes (10 mM in DI water) respectively, and the fiber outlet was placed into 400 µl of 10 mM KCl(aq) solution. A constant 1 V potential was applied to the source electrode for 17 hours, with the target system grounded and simultaneously the resulting current was measured. Then the system was operated applying 1.7 µA (0.5 mC) every 5 min for 30 minutes for 10 mM SA (aq) source electrolyte. At the final electrical characterization step, the system was operated applying different currents (10 nA, 50 nA, 100 nA, and 200 nA) between the source and target electrodes for 1.5, 3, 6, and 20 hours for SA source electrolyte while the voltage was measured. The devices were operated in a target solution of 10 mM KCl(aq). The electrical characterization was repeated replacing the KCl target electrolyte with a human primary cell solution applying a constant current of 10 nA for 17 hours or 6 nA for 6 hours. A custom-made “source-meter” with custom LabVIEW software was used to deliver SA to the monocytes.

Quantification of ASA and SA in the target electrolyte

The target solutions were collected after the ASA and SA delivery, and the amount of delivered molecules were measured using a salicylate enzyme-linked immunosorbent assay (ELISA) kit (Neogen) measured on a BioTek Synergy H1m plate reader according to the manufacturer's instructions.

UV analysis

A UV/Vis/NIR spectroscopy (PerkinElmer Instruments Lambda 900 and a home-built setup) with 1 cm quartz cells was used, and spectra were collected from 240 to 400 nm.

Cell culture and LPS stimulation

Peripheral blood mononuclear cells (PBMCs) were isolated from buffy coats obtained from healthy individuals (from Linköping Blood Bank, Linköping, Sweden) who had given written consent for research use of the donated blood in accordance with the Declaration of Helsinki and paragraph 4 of the Swedish law (2003:460) on Ethical Conduct in Human Research. PBMC separation from buffy coats were performed by density gradient centrifugation on Lymphoprep (Axis-Shield, Oslo, Norway) as previously described[47], and isolation of monocytes from the PBMCs was performed by negative selection using the Human Monocyte Enrichment Kit without CD16 Depletion according manufacturer instructions (STEMCELL Technologies, Grenoble, France). The isolated monocytes were kept in DMEM cell culture medium supplemented with 10% pooled natural human serum (Linköping Blood Bank). 200 000 monocytes in 400 µl cell culture medium was aliquoted to each 1.5 ml polypropylene Eppendorf tube and placed in a 37 °C incubator. Lipopolysaccharides (LPS) from *Escherichia coli* O26:B6 (L3755, Sigma) were diluted in cell culture medium supplemented as stated above and used to stimulate monocytes for the different periods indicated. The dose of LPS was selected by titration and deemed appropriate based on a robust response from the monocytes that peaked 6 h, and that was moderately inhibited by SA when added together with LPS. When the capillary OEIPs were used to deliver SA to the monocytes (for 6 or 17 h prior LPS-stimulation), the sampling of the cell culture medium was performed before and after the 6 h LPS-stimulation. Clearing of cell culture supernatants were performed by one 5 000 g centrifugation and the cleared supernatants were stored at -80 °C until assayed.

Quantification of TNFα and IL-6 released from monocytes

Basal levels (before stimulation) and LPS-induced levels (after stimulation) of the pro-inflammatory cytokines TNFα and IL-6 were assayed from the cell-free culture medium (cleared supernatants). Quantification of TNFα and IL-6 levels were determined by cytometric bead array analysis according to the manufacturer's protocol (BD Biosciences) as previously described[48], and data acquired using a Gallios flow cytometer (Beckman Coulter, Brea, CA). Cytokine concentrations based on a standard curve were analyzed using FlowJo version 10.5.3 and Microsoft Excel.

Statistical analysis

Once the OEIP delivery device were characterized, delivery efficiency confirmed, and the experimental parameters set, the biological usefulness of OEIP-delivered SA to inflammatory monocytes was evaluated. For this purpose, GraphPad Prism (version 5) was used to perfoerm a two-sided repeated-measures ANOVA with the post hoc Tukey multiple comparison test to compare the groups, without pre-processing of data and without any adjustments. p values <0.05 were considered significant.

Conclusions

In this work, we successfully fabricated free-standing OEIP devices within a capillary fiber form factor for inflammation treatment in monocytes – the first use of such capillary OEIPs with mammalian cells. This design offers several advantages for use with implantable OEIP devices since the capillary fiber serves as both encapsulation and substrate and can easily be implanted or positioned in the proximity of specifically targeted cells. In this study, capillary OEIPs were arranged in the proximity of inflammatory monocytes and local delivery of salicylic acid (SA) was initiated. Highly localized SA delivery completely abolished the rise in pro-inflammatory cytokine (TNFα and IL-6) levels after LPS stimulation with low dosage, preventing the activation of inflammatory monocytes. These results demonstrate a useful approach to optimize transport and local and specific delivery of different therapeutic substances, at low doses for implantable OEIP applications with limiting side effects. In the future one can envision an integrated implantable device including sensing functionality (probing for levels of inflammation[49]) as well as therapeutic delivery of anti-inflammatory drugs (such as SA). Such

technology would allow for delivery of therapeutics to be tailored to fit the unique inflammatory response of each patient while keeping the amount of delivered drug to the minimum level needed.

Supporting Information Description

Charge distribution for ASA and SA depends on pH; Figure S1.

Author Contributions

Maria Seitanidou carried out the experiments, fabricated and characterized the devices, and wrote the manuscript. Robert Blomgran performed the culture of cells, LPS stimulations, and cytokine measurements. Giggil Pushpamithran performed monocyte isolations. Magnus Berggren and Daniel T. Simon supervised the project. All authors discussed the results and contributed to the final manuscript.

Acknowledgements

The authors wish to thank Dr. Erik Gabrielsson and Dr. David Poxson for their assistance in designing devices, and Meysam Karami Rad for his assistance in designing and developing a mobile sourcemeter for the cell experimenters in the incubator. This work was primarily supported by the Swedish Foundation for Strategic Research. Additional funding was provided by the Advanced Functional Materials SFO-center at Linköping University, the Önnesjö Foundation, and the Knut and Alice Wallenberg Foundation.

Conflict of interest

D.T.S. and M.B. are shareholders in the small, researcher-controlled intellectual property company OBOE IPR AB (oboeipr.com), which owns patents related to OEIPs.

References

[1] J. Isaksson, P. Kjäll, D. Nilsson, N. Robinson, M. Berggren, A. Richter-Dahlfors, *Nat. Mater.* 2007, *6*, 673.

[2] G. G. Malliaras, *Biochim. Biophys. Acta - Gen. Subj.* 2013, *1830*, 4286.

[3] R. M. Owens, G. G. Malliaras, *MRS Bull.* 2010, *35*, 449.

[4] T. Someya, Z. Bao, G. G. Malliaras, *Nature* 2016, *540*, 379.

[5] D. T. Simon, E. O. Gabrielsson, K. Tybrandt, M. Berggren, *Chem. Rev.* 2016, *116*, 13009.

[6] D. T. Simon, K. C. Larsson, D. Nilsson, G. Burström, D. Galter, M. Berggren, A. Richter-Dahlfors, *Biosens. Bioelectron.* 2015, *71*, 359.

[7] L. Torsi, M. Magliulo, K. Manoli, G. Palazzo, *Chem. Soc. Rev.* 2013, *42*, 8612.

[8] J. T. Mabeck, G. G. Malliaras, *Anal. Bioanal. Chem.* 2006, *384*, 343.

[9] A. Dodabalapur, *Mater. Today* 2006, *9*, 24.

[10] N. Lago, A. Cester, *Appl. Sci.* 2017, *7*, 1292.

[11] L. Ricotti, A. Cafarelli, V. Iacovacci, L. Vannozzi, A. Menciassi, *Curr. Nanosci.* 2015, *11*, 144.

[12] C. Boehler, M. Asplund, *J. Biomed. Mater. Res. - Part A* 2015, *103*, 1200.

[13] R. Wadhwa, C. F. Lagenaur, X. T. Cui, *J. Control. Release* 2006, *110*, 531.

[14] T. Arbring Sjöström, M. Berggren, E. O. Gabrielsson, P. Janson, D. J. Poxson, M. Seitanidou, D. T. Simon, *Adv. Mater. Technol.* 2018, *3*, DOI 10.1002/admt.201700360.

[15] X. Strakosas, J. Selberg, Z. Hemmatian, M. Rolandi, *Adv. Sci.* 2017, *4*, 1.

[16] C. Z. Yingxin Deng, Erik Josberger, Jungho Jin, Anita Fadavi Rousdari, Brett A. Helms, M. P. Anantram and Marco Rolandi, *Sci. Rep.* 2013, 1.

[17] A. Jonsson, Z. Song, D. Nilsson, B. A. Meyerson, D. T. Simon, B. Linderoth, M. Berggren, *Sci. Adv.* 2015, *1*, e1500039.

[18] J. Isaksson, D. Nilsson, P. Kja, N. D. Robinson, A. Richter-dahlfors, M. Berggren, 2008, *9*, 303.

[19] D. T. Simon, S. Kurup, K. C. Larsson, R. Hori, K. Tybrandt, M. Goiny, E. W. H. Jager, M. Berggren, B. Canlon, A. Richter-Dahlfors, *Nat. Mater.* 2009, *8*, 742.

[20] E. O. Gabrielsson, K. Tybrandt, P. Hammarström, M. Berggren, K. P. R. Nilsson, *Small* 2010, *6*, 2153.

[21] A. Jonsson, S. Inal, I. Uguz, A. J. Williamson, L. Kergoat, J. Rivnay, D. Khodagholy, M. Berggren, C. Bernard, G. G. Malliaras, D. T. Simon, *Proc. Natl. Acad. Sci.* 2016, *113*, 9440.

[22] A. Williamson, J. Rivnay, L. Kergoat, A. Jonsson, S. Inal, I. Uguz, M. Ferro, A. Ivanov, T. A. Sjöström, D. T. Simon, M. Berggren, G. G. Malliaras, C. Bernard, *Adv. Mater.* 2015, *27*, 3138.

[23] C. M. Proctor, A. Slézia, A. Kaszas, A. Ghestem, I. del Agua, A.-M. Pappa, C. Bernard, A. Williamson, G. G. Malliaras, *Sci. Adv.* 2018, *4*, eaau1291.

[24] D. J. Poxson, M. Karady, R. Gabrielsson, A. Y. Alkattan, A. Gustavsson, K. Ljung, M. Grebe, D. T. Simon, M. Berggren, *Proc. Natl. Acad. Sci.* 2017, accepted.

[25] I. Bernacka-Wojcik, M. Huerta, K. Tybrandt, M. Karady, Y. Mulla, D. J. Poxson, E. Gabrielsson, M. Berggren, D. T. Simon, E. Stavrinidou, *Small* 2019, (submitted).

[26] D. J. Poxson, E. O. Gabrielsson, A. Bonisoli, U. Linderhed, T. Abrahamsson, I. Matthiesen, K. Tybrandt, M. Berggren, D. T. Simon, *ACS Appl. Mater. Interfaces* 2019, *11*, 14200.

[27] M. Seitanidou, K. Tybrandt, M. Berggren, D. T. Simon, *Lab Chip* 2019, *19*, 1427.

[28] H. Strathmann, *Ion-Exchange Membrane Separation Processes*, Elsevier, 2004.

[29] K. Schör, *Acetylsalicylic Acid*, Wiley-VCH Verlag GmbH & Co. KGaA, 2016.

[30] P. C. E. Golia,G. Limongelli, F. Natale,F. Fimiani, V. Maddaloni, I. Pariggiano, R. Bianchi, M. Crisci, L. D'Acierno, R. Giordano, G. Di Palma, M. Conte, P. Golino, M. G. Russo, R. Calabrò, *Springer Sci.* 2014, *16*, 435.

[31] L. Chen, H. Deng, H. Cui, J. Fang, Z. Zuo, *Oncotarget* 2017.

[32] J.R.N. Nansseu, J.J.N. Noubiap, *Tromb J.* 2015, *13*, 38.

[33] J.E Dalen, *Am J Med* 2006, *119*, 198.

[34] M. H. etc Hiroshi Sato;Kinji Ishikawa, *Stroke* 2006, *37*, 447.

[35] Hirsh Jack, *New Engl Reg Allergy Proc* 1981, *2*, 83.

[36] T. Krakauer, *Clin. Diagn. Lab. Immunol.* 2002, *9*, 126.

[37] T. Hochdörfer, C. Tiedje, D. J. Stumpo, P. J. Blackshear, M. Gaestel, M. Huber, *Cell. Signal.* 2013, *25*, 1339.

[38] C. M. Moore, N. L. Akers, A. D. Hill, Z. C. Johnson, S. D. Minteer, 2004, 1241.

[39] J. Dong, J. Li, L. Cui, Y. Wang, J. Lin, Y. Qu, H. Wang, *BMC Vet. Res.* 2018, 1.

[40] M. Yin, Y. Yamamoto, R. B. Gaynor, *Nature* 1998, *396*, 77.

[41] H. and G. Xueqin Li , Jun Shen , Yunyao Jiang, Ting Shen, Long You, Xiaobo Sun, Xudong Xu, Weicheng Hu, *Int. Mol. Sci* 2016, *17*, DOI 10.3390/ijms17111938.

[42] M. Seitanidou, J. F. Franco-Gonzalez, T. Arbring, I. Zozoulenko, M. Berggren, D. T. Simon, T. A. Sjöström, I. Zozoulenko, M. Berggren, D. T. Simon, *J. Phys. Chem. B* 2017, *121*, 7284.

[43] O. A. Contents, M. Rattana, N. Paradee, A. Sirivat, S. Niamlang, T. Petroleum, M. Engineering, T. Thanyaburi, T. Petroleum, *Int. J. Drug Dev. Res.* 2015, *7*, 107.

[44] M. Houshmand, A. Jabbari, H. Heli, M. Hajjizadeh, *J Solid State Electrochem* 2008, *12*, 1117.

[45] G. Murtaza, S. A. Khan, A. Shabbir, A. Mahmood, H. Hassan, B. Asad, K. Farzana, N. S. Malik, I. Hussain, 2011, *6*, 417.

[46] J. Courtois, M. Szumski, E. Byström, A. Iwasiewicz, A. Shchukarev, K. Irgum, *J. Sep. Sci.* 2006, *29*, 14.

[47] A. M. Andersson, B. Andersson, C. Lorell, J. Raffetseder, M. Larsson, R. Blomgran, *Sci. Rep.* 2016, *6*, 1.

[48] S. K. Singh, A. M. Andersson, R. Ellegård, C. S. Lindestam Arlehamn, A. Sette, M. Larsson, O. Stendahl, R. Blomgran, *Am. J. Pathol.* 2016, *186*, 3083.

[49] C. Diacci, M. Berto, M. Di Lauro, E. Bianchini, M. Pinti, D. T. Simon, F. Biscarini, C. A. Bortolotti, *Biointerphases* 2017, *12*, 05F401.